JOURNAL OF PROPULSION AND POWER
Vol. 23, No. 6, November–December 2007

Effect of Hot-Streak Counts on Turbine Blade Heat Load and Forcing

L. He* and V. Menshikova†
University of Durham, Durham, DH1 3LE England, United Kingdom
and
B. R. Haller‡
Siemens Industrial Turbomachinery, Ltd., Lincoln, LN5 7FD England, United Kingdom

DOI: 10.2514/1.29603

A computational analysis is carried out on the influence of turbine inlet temperature distortion (hot streaks) from both blade aeromechanical (forced vibration) and aerothermal (heat transfer) viewpoints. Analysis of hot streaks with variable circumferential lengths, corresponding to different numbers of combustion burners, shows that the circumferential wavelength of the temperature distortion can significantly change unsteady forcing and the heat load on rotor blades. When the hot-streak wavelength is the same as the nozzle-guide-vane blade pitch, there is a strong dependence of the preferential heating on the relative clocking position between the hot streak and nozzle-guide-vane blade. However, this clocking dependence is shown to be qualitatively weakened for the cases with fewer hot streaks with longer circumferential wavelengths.

Nomenclature

C	=	blade axial chord
h	=	spanwise distance
P	=	pressure
T	=	temperature
To	=	stagnation temperature

Subscripts

av	=	time-averaged value
isen	=	isentropic
1	=	inlet

I. Introduction

THE performance of aeroengines and gas turbines is crucially influenced by the turbine inlet temperature. An important issue to be considered during design is the nonuniform gas temperature profile supplied to the HP turbine inlet due to circumferential discrete combustion burners. Nonuniform inlet temperatures (hot streaks) can have effects on HP turbine aerothermal performance (load and efficiency), blade heat transfer, and blade aeromechanics (forced vibration/response). Basic understanding of the kinematic behavior of hot streaks and impacts is based on the work on general turbomachinery unsteady wake transportation by Kerrebrock and Mikolajczak [1]. The hot streaks cause significant heat load on the HP turbine rotor blades; in particular, rotor pressure surfaces tend to be heated further. This so-called preferential heating is due to an enhanced cross-passage fluid movement from the suction surface to the pressure surface in a hot portion of the gas, due to an increased incidence. This is confirmed experimentally by Butler et al. [2] and computationally by Dorney et al. [3] and Krouthen and Giles [4]. A further change of the heating effect can result from the potential nozzle-guide-vane (NGV)–rotor interaction and, as such, the heating on rotor blades can be reduced by the choice of NGV/rotor blade count ratio, as reported by Shang and Epstein [5]. Sondak et al. [6] also showed a considerable dependence of the heating on the NGV/rotor blade count.

In a turbine stage, the high-loss fluid within a wake shed from the upstream relatively rotating row will be convected from the pressure to the suction surface; this is the so-called negative jet. Similarly, the cross-passage movement within a hot streak can be regarded as a positive jet. These two opposing movements can suppress each other. Thus, the lossy fluid in a wake will be less likely to be accumulated on the suction side, and the high-temperature fluid in a hot streak will be less likely to be accumulated on the pressure side. This phasing between the two leads to the clocking dependence of the preferential heating effects, as studied by Dorney and Gundy-Burlet [7] and Takahashi et al. [8]. Apart from blade heat transfer, the effects on blade aeromechanics (forced response) will also need to be considered during design. The work by Manwaring and Kirkeng [9] clearly showed that a temperature distortion at the turbine inlet can go through a multistage turbine and generate large unsteady forcing and thus blade vibratory response, even in the last stage of the low-pressure turbine in a realistic aeroengine configuration.

A particular aspect of interest is the circumferential wavelength of the hot streak (hot-streak count). Most of the previous studies on the clocking (indexing) effect adopt a hot-streak/NGV count ratio of 1:1. In realistic engine combustion configurations, the number of combustors/burners tends to be much smaller than that of the NGV blades. The aerodynamic loss characteristics of a multistage turbine subject to highly distorted inlet flows due to a partial admission are shown to be strongly dependent on the distortion circumferential wavelength [10]. Therefore, it would be of interest to clarify the issue for situations with the temperature distortions. The results should offer some guidance on the applicability of the findings based on an equal hot-streak/NGV count; they should also be relevant to the design choice of the number of combustors/burners and cooling arrangements.

II. Computational Method and Turbine Test Case

The method used in the present study is a three-dimensional unsteady Navier–Stokes solver developed and validated at Durham University, particularly for turbomachinery unsteady aerodynamics and aeromechanics applications (e.g., [11–13]). The flow equations are solved numerically in a cylindrical coordinate system. For the turbulence closure, the option of the Baldwin–Lomax mixing-length model is adopted in the present studies. Some initial test calculations

Received 5 January 2007; revision received 29 May 2007; accepted for publication 6 June 2007.

*Professor of Thermofluids, School of Engineering.
†Research Associate, School of Engineering.
‡Turbine Technology Manager.

are carried out using the Spalart–Allmaras one-equation model, giving very small differences in terms of the blade surface pressures and temperature distributions compared with those using the mixing-length model. The governing equations are discretized in space using a cell-centered finite volume scheme, together with the Jameson-type blend of second- and fourth-order artificial dissipation to damp numerical oscillations. The baseline temporal integration of the discretized equations is carried out using the explicit four-step Runge–Kutta scheme. The explicit time-marching scheme is subject to a limitation on the length of time step due to the numerical stability requirement, and this is very restrictive on unsteady viscous flow calculations. This difficulty can be overcome by using the solver options of dual time stepping [14] and the time-consistent multigrid [11].

The computations are carried out in a multipassage and multirow domain, as shown in Fig. 1 for a midspan section of a turbine stage. The relatively moving rotor and stator meshes are patched together at the interface. There are two options for the interface treatment. The steady flow multiple-row solution is obtained by using the mixing-plane technique. At each spanwise section, the mixed-out variables at both the rotor and stator sides are flux-averaged. The difference in the mixed-out variables across the interface represents a jump in characteristics. The procedure is to drive characteristic jumps to zero in a nonreflective manner. The second method is for unsteady flow calculations. A second-order interpolation and correction method enables local instantaneous information to be transferred directly across the interface.

On blade/endwall surfaces, the log law is applied to determine the surface shear stress, and the tangential velocity is left to slip. This slip wall condition is preferred for unsteady 3-D multipassage calculations because of the relatively coarse meshes to be used. For the present HP turbine case, the overtip leakage effect is not included. For the energy equation, the adiabatic wall condition is applied. This means that the heat transfer between the fluid and the surface is not included. It is recognized that this will introduce errors in calculated surface temperature distributions. But because the cross-passage migration and redistribution of the temperature field associated with the influence of hot streaks are largely determined by the corresponding fluid kinematics, the use of the adiabatic wall condition should not have significant bearing in the qualitative characteristics of rotor blade heat loads caused by different hot-streak configurations considered here. It is acknowledged that more refined solutions can be obtained with inclusion of tip-clearance modeling and use of nonslip wall conditions (hence much finer meshes), but it is not expected that the main outcomes of the present study will be changed, given the spatial and temporal length scales of the disturbances of interest.

At the circumferential periodic boundaries, the direct periodic (repeating) condition is used in the present study. This means that the numbers of rotor and stator passages included in the domain need to have the same total circumferential length. At the inlet, stagnation parameters and flow angles are specified. The detailed inlet stagnation temperature profiles will be described later. At the exit, the pitchwise mean static pressure at each spanwise section is specified, and the local upstream-running characteristic is formulated to drive the pitchwise average pressure to the specified value, whereas the local pitchwise nonuniformity is determined by the downstream-running characteristic.

The test configuration used in the present study is a transonic HP turbine stage MT1, as described by Chana et al. [15]. The rotation speed is 9500 rpm and the calculated stage pressure ratio is about 2.8. The turbine stage has 32 NGV blades and 60 rotor blades. Initial calculations are conducted using the mixing-plane option, which needs only one NGV passage and one rotor passage. The unsteady stage computations are carried out in a multipassage domain. For this case, the domain needs to contain 8 NGV blade passages and 15 rotor blade passages to enable the direct periodic/repeating condition to be applied at the circumferential boundaries. A mesh density of $40 \times 77 \times 40$ per NGV passage and $40 \times 89 \times 40$ per rotor passage is used, giving 3.12 million grid points for the total of 23 passages. Based on some preliminary test on the mesh dependency for steady flow solutions for this case and on previous mesh-dependency studies for a turbine stage for the same solver [11], the mesh density is judged to be sufficient for the present study. Figure 1 shows the stage mesh views on a blade-to-blade section and on a meridional plane.

The first set of calculations is carried out at a uniform inlet stagnation temperature of 444 K, a uniform inlet stagnation pressure 460 kPa, and an exit static pressure 142.8 kPa. A well-established periodic solution can be obtained in three beating periods (1500 time steps for each beating period, which covers 15 rotor blade passing periods and 8 NGV blade passing periods) when a multipassage unsteady computation is started from a single-passage steady mixing-plane solution.

Figure 2 shows the NGV blade surface isentropic Mach number distributions at the midspan in comparison with the time-averaged experimental data [15]. The calculated results are those from a pure steady flow solver (the mixing-plane treatment) and the time-averaged results of the unsteady simulation. The unsteady potential interaction between the NGV and rotor should mainly affect the region near the NGV trailing edge, and this is the area in which we can see some clear difference between the steady and unsteady

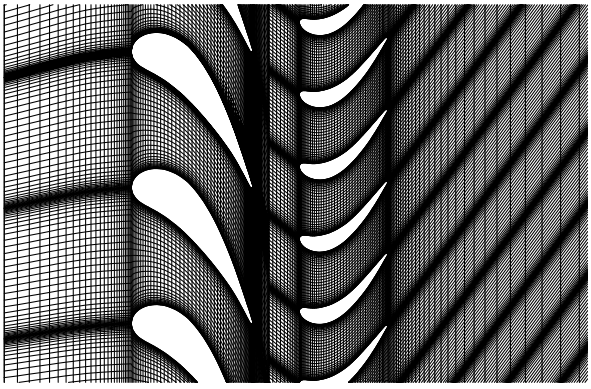

a) Blade–blade view (midspan section)

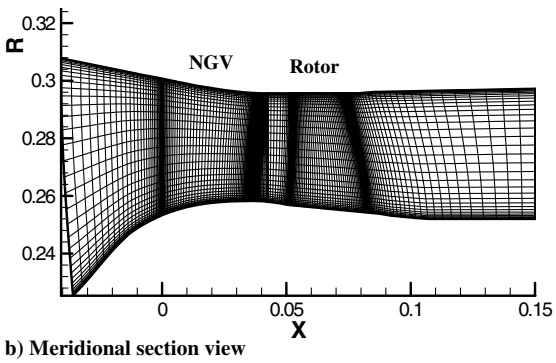

b) Meridional section view

Fig. 1 Computational mesh for a turbine stage.

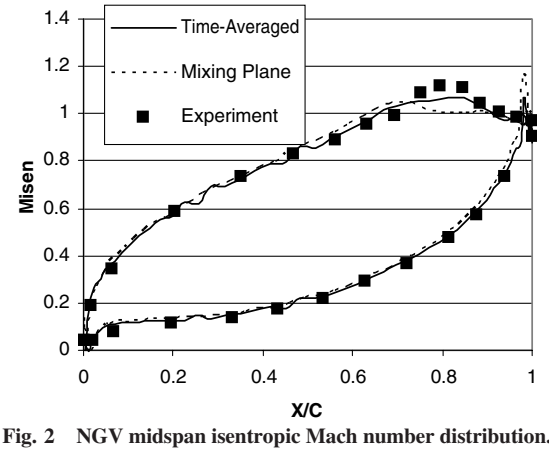

Fig. 2 NGV midspan isentropic Mach number distribution.

solutions. The unsteady result is closer to the experimental data than the steady result. In particular, at around 80% chord on the suction surface, the unsteady solution produces a larger supersonic region, similar to that in the experiment, whereas the oblique trailing-edge shock from the mixing-plane solution hits the suction surface farther upstream. The trailing-edge overshoot of the pressure on the pressure surface is much reduced in the unsteady result. Following a typical flow pattern around a turbine blade trailing edge, both of these two features seem to imply that the NGV exit flow angle predicted by the steady mixing-plane treatment would be smaller (hence less turning) than the time-averaged value from the unsteady solution. Overall, the comparison between the unsteady solution and the experimental data for the NGV is very good.

For the rotor, the result at the rotor midspan section is not as good as that for the NGV blade, as shown in Fig. 3. The pressures are all normalized by the maximum surface pressure corresponding to the rotor stagnation pressure, and thus the unit isentropic Mach number corresponds to a $P/P_{\max}$ value of 0.528. The calculated surface pressures for most of the suction surface are higher than the experimental data. Nevertheless, the time-averaged unsteady calculation is closer to the experimental data than the steady mixing-plane solution. Compared with the mixing-plane results, the time-averaged unsteady flowfield around the rotor seems to be subject to a higher incidence, as indicated by the pressure distribution over the frontal part of the suction surface. This is in line with the higher turning provided by the NGV in the unsteady calculations discussed earlier.

The calculated unsteady pressure variations are compared with the experimental data, as shown in Figs. 4 and 5. The results are for the unsteady pressures at three different chordwise locations of the rotor blade midspan section, normalized by the corresponding local time-averaged values. The reference phase angle is chosen to match the calculated phase with the experimental value for the leading edge on the suction surface.

The highest unsteady pressures are around the frontal part of the suction surface. The large phase change (higher than 180 deg) between the leading edge and 51% chord indicates that the suction-surface pressure variation is dominated by the sweep of the NGV trailing-edge shock wave, typical of transonic turbine stages (e.g., Miller et al. [16]). The pressure side is, on the other hand, not so directly affected by the NGV shock wave. The unsteady pressure amplitudes change much less along the chord, and the slight phase lead in the rear part of the pressure surface indicates that the local flow is subject to the upstream propagation of reflected waves. Overall, the calculated magnitudes and relative phase angles of unsteady pressures compare well with the experimental data.

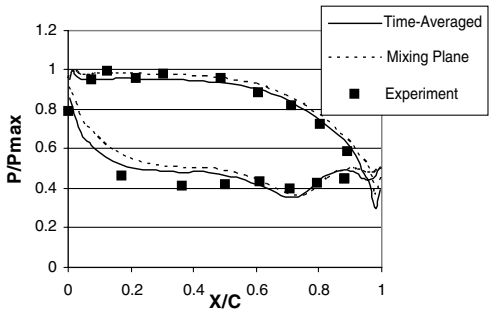

Fig. 3 Rotor midspan surface static pressure distribution.

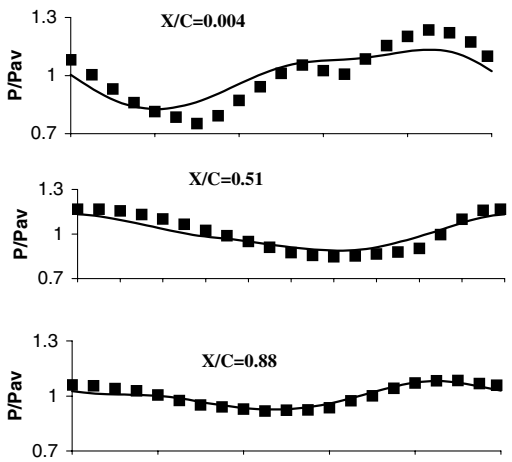

Fig. 4 Unsteady pressures at different chordwise positions (suction surface): calculation (line) and experiment (■).

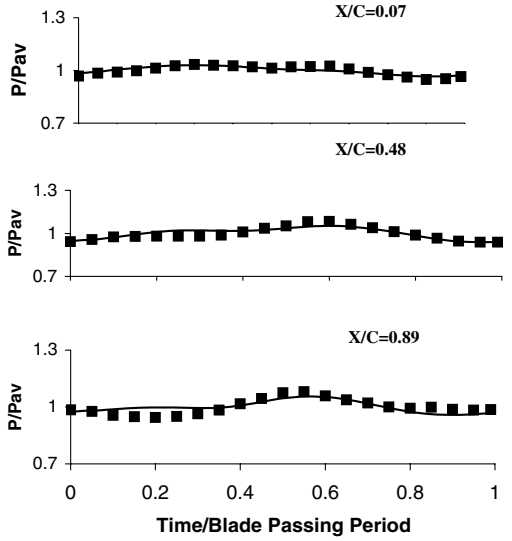

Fig. 5 Unsteady pressures at different chordwise positions (pressure surface): calculation (line) and experiment (■).

III. Analysis of Inlet Temperature Distortion (Hot Streak)

For the hot-streak calculations, stagnation temperature profiles are specified at the inlet to the computational domain. The main interest here is to analyze the influence of the circumferential wavelength of the hot streaks. The results for two different hot-streak configurations (32 and 8 hot streaks) are presented here. The computational domain containing one-fourth of the annulus therefore has eight or two hot streaks, as shown in Fig. 6. The stagnation temperature profile is chosen with the same sinusoidal radial distribution of the pitchwise mean value, as shown in Fig. 7. At each span section, the stagnation temperature also varies in a sinusoidal fashion in the circumferential direction, according to a given wavelength (number of hot streaks). For all of the cases calculated, the minimum value of the stagnation temperature is taken to be 400 K and the maximum is 600 K. Hence, the peak temperature ratio at the inlet is $To_{\max}/To_{\min} = 1.5$.

This temperature ratio is typical of those used in previous studies on the hot-streak effects. The overall averaged value at the inlet closely matches that for the uniform inlet case presented earlier. It should be mentioned that combustion exit temperature distortions are typically measured in terms of the radial temperature distribution factor (RTDF)

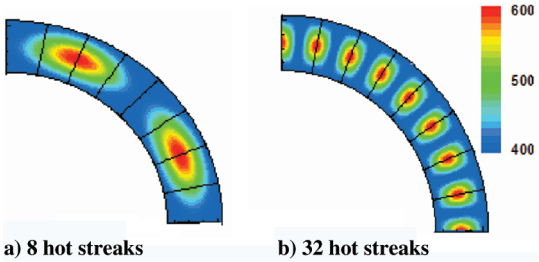

Fig. 6 Inlet stagnation temperature profile (one-fourth annulus).

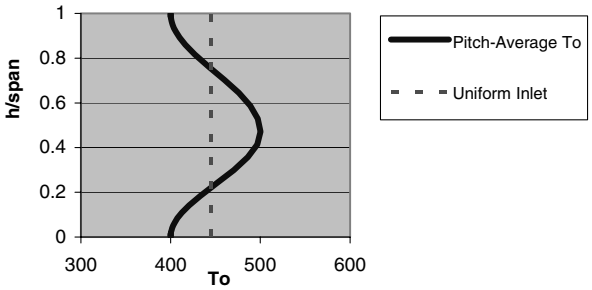

Fig. 7 Spanwise variation of pitch-averaged stagnation temperature at the inlet.

$$\text{RTDF} = \frac{\bar{T}o_{\text{pitch}} - \bar{T}o_{\text{overall}}}{\bar{T}o_{\text{overall}} - To_{\text{combustor entry}}} \tag{1}$$

and the overall temperature distribution factor (OTDF):

$$\text{OTDF} = \frac{To_{\max} - \bar{T}o_{\text{overall}}}{\bar{T}o_{\text{overall}} - To_{\text{combustor entry}}} \tag{2}$$

In the present cases with different numbers of hot streaks, the pitchwise averaged value $\bar{T}o_{\text{pitch}}$, the maximum value $To_{\max}$, and the overall averaged value $\bar{T}o_{\text{overall}}$ are kept the same. Hence, the two cases should have the same OTDF and RTDF values, regardless of the number of hot streaks and the corresponding wavelength.

A. Rotor Surface Temperatures (32 Hot Streaks)

The calculations are first conducted for 32 hot streaks, corresponding to Fig. 6b. Note that the number of NGV blades is also 32. The hot-streak configuration with the same hot-streak/NGV blade count is widely used in previous studies, in particular, with respect to the hot-streak/NGV clocking effects. It is useful to adopt this configuration first to compare the present results with those from the previous work, before looking at the effects of different hot-streak wavelengths. For high-speed turbines, the temperature migration due to the hot streak can be clearly traced in terms of contours of entropy due to its convective nature. The midspan instantaneous entropy contours for the case with the inlet hot streaks located at the midpassage of NGV blades are shown in Fig. 8a. Those with the hot streaks impinging on the NGV blade leading edge are shown in Fig. 8b.

For a typical stator–rotor stage without an inlet hot streak, high-entropy fluid of wake shed from the NGV will be accumulated on the rotor suction surface, due to a pressure-surface-to-suction-surface cross-passage-movement negative jet. However, for a case subject to a nonuniform temperature field, the opposite happens within a hot streak, due to an extra relative velocity caused by heating. Consequently, the hot fluid with high entropy would tend to be convected toward the pressure surface. This so-called preferential heating is clearly identifiable by the high-entropy fluid (in red) accumulated on the rotor pressure surface (Fig. 8a). The NGV midpassage hot streak gives the strongest preferential heating effect, because the two opposing cross-passage movements are now completely out of phase. The negative jet convects the lossy fluid in a NGV wake to the suction side without strongly interacting with the positive jet, which convects the hot fluid toward the pressure side. It then follows that the preferential heating should be considerably hindered when the hot streaks are impinged on the NGV blades. Now the hot streaks are in phase with the NGV wakes. The net cross-passage movement will depend on relative strengths of the two opposing mechanisms. For the present case, the temperature difference is quite high, and so the cross-passage movement is still determined by the positive jet. However, the preferential heating is seemingly weakened (Fig. 8b). The hot-fluid accumulation on the pressure surface now is not easily identifiable.

The pressure surface temperature distributions on rotor blades at 10, 50, and 90% span sections are shown in Fig. 9. Consider the time-

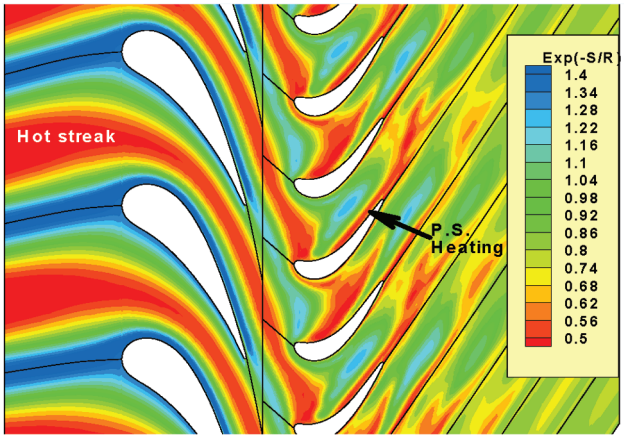

a) Hot streak located at NGV midpassage

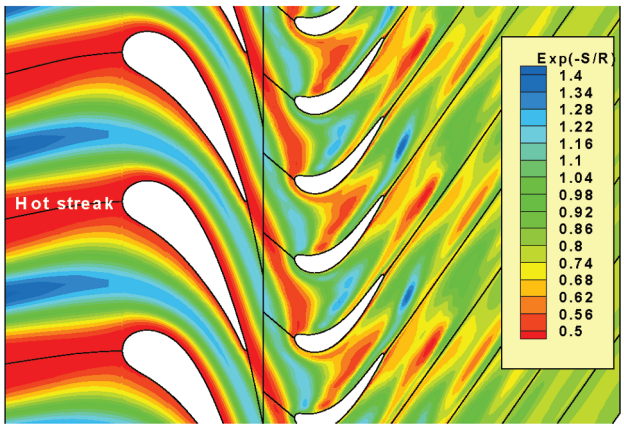

b) Hot streak impinging at NGV leading edge

Fig. 8 Instantaneous entropy contours at midspan section.

averaged temperatures around the leading edge of the rotor blades. The rotor leading-edge region should not be affected by the rotor cross-passage movement and the preferential heating mechanism. Thus, at both hub and casing, the time-averaged rotor inlet temperatures for the two hot-streak cases would be expected to be lower than those of the uniform inlet case (see Fig. 7). The leading-edge temperatures for the hot streaks located in the NGV midpassage follow the expected trend. For the impinging hot-streak case, however, the temperature follows the expected variation only at 90% span (Fig. 9c). At the midspan (Fig. 9b), the rotor leading-edge temperatures for the two hot-streak cases are noticeably different. Near the hub at 10% span (Fig. 9a), the temperature of the impinging hot-streak case is even higher than that of the uniform inlet. This might well be attributed to the radial migration of hot streaks occurring within the NGV. The spanwise location of hot streaks as they leave the NGV would depend on the NGV/hot-streak clocking. NGV blade suction-surface temperature contours (as shown in Fig. 10) indicate that when hot streaks impinge on the NGV blades, the fluid within a hot streak is radially shifted from the midspan toward the hub section over the rear part of the NGV blades.

The radial pressure gradient required to maintain the swirl at the NGV exit would drive the low-momentum fluid in the blade boundary layer and wakes to move inward. It is of interest to note that the flow visualization for the NGV blade under a uniform flow condition [17] also indicates a shift of the suction-surface streamline pattern from the casing to the hub. Hence, the hot fluid will also be convected radially inward by the NGV secondary flow of this kind if the hot streak impinges on the NGV blade. Consequently, the temperature for the impinging hot-streak case is much higher than that of the midpassage hot-streak case around the rotor leading edge at 10% span (Fig. 9a). The radially inward migration in the NGV row by the secondary flow mechanism should also lead to a relatively

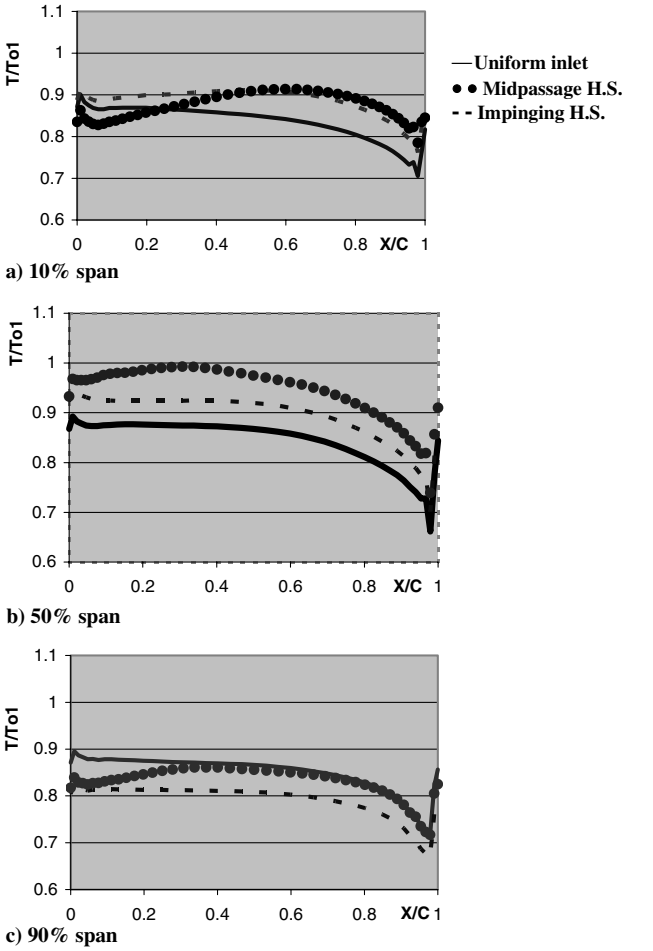

Fig. 9 Time-averaged temperatures at three spanwise sections of the rotor pressure surface [32 hot streaks (H.S.)].

lower rotor temperature around the leading edge at the midspan for the impinging hot-streak case (Fig. 9b).

Overall, the cases with 32 hot streaks show a strong dependence on the clocking between the hot streaks and the NGV blades. The key is the phasing among several fluid kinematic features, with both temporal and spatial length scales being the NGV blade passage. The results for unsteady surface pressures and blade forces presented later will also show that for this case, the hot streaks have a relatively small influence on the rotor passage flow in a dynamic sense.

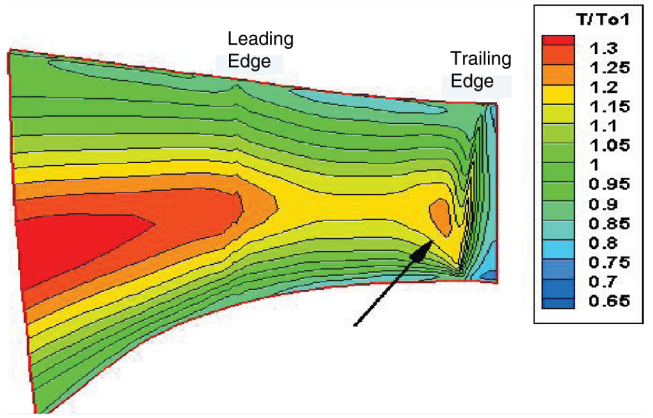

Fig. 10 Temperature contours on a meridional mesh surface, overlapping with NGV suction surface (hot streak impinging at the NGV leading edge).

B. Rotor Surface Temperatures (Eight Hot Streaks)

When the number of hot streaks is reduced to eight, the circumferential wavelength is increased by a factor of 4. Again, two hot-streak/NGV clocking positions are considered. The case with hot streaks impinging on the NGV blades is as shown in Fig. 6a. Similar to the 32-hot-streak case, a midpassage hot-streak situation is achieved by circumferentially shifting the temperature profile by half of a NGV blade pitch. The calculated time-averaged temperatures on the rotor blade pressure surface at 10, 50, and 90% span sections are shown in Fig. 11. The results for this long-wavelength case are qualitatively different from those for 32 hot streaks. The time-averaged surface temperatures are almost identical, showing no dependence on the hot-streak/NGV clocking position. Looking at the unsteady temperatures in terms of the maximum and minimum values, we also see only very small differences between the two hot-streak clocking positions (Fig. 12).

The insensitivity of rotor surface temperatures to the hot-streak clocking for the eight-hot-streak case is directly attributed to the difference in the length scale between the hot streak and the NGV blade passage. Basically, the rotor is now subject to two temporal disturbances: 1) the aerodynamic disturbance from the NGV and 2) the NGV-modulated hot streaks. For the 32-hot-streak cases, both disturbances have the same temporal and spatial frequencies. As such, the phasing between the two in terms of the corresponding kinematics can either enhance or reduce the cross-passage movement and migration. But for the eight-hot-streak case, a phasing between two disturbances at different frequencies no longer matters.

A further comparison is made between the eight-hot-streak case and that with 32 hot streaks for the clocking position when the hot streak is placed at the NGV midpassage. The time-averaged temperatures are given in Fig. 13. The maximum and minimum unsteady temperatures are shown in Fig. 14. Because the temperature field of a hot streak can no longer be phased in relation to the NGV velocity field, the eight-hot-streak case gives a noticeably reduced preferential heating. The time-averaged temperature is about 5% lower than that of 32 hot streaks for most of the pressure surface (Fig. 13).

On the other hand, the peak-to-peak unsteady temperature variation for the eight-hot-streak case is roughly three times larger than that in the 32-hot-streak case (Fig. 14), although both cases have

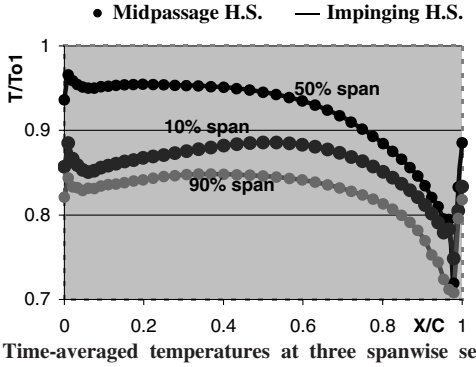

Fig. 11 Time-averaged temperatures at three spanwise sections of rotor pressure surface (eight hot streaks).

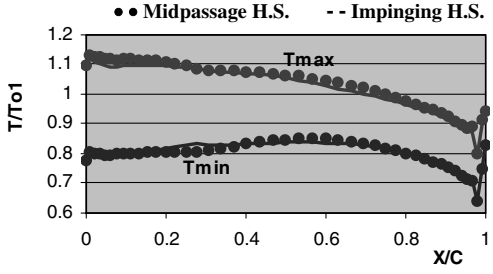

Fig. 12 Maximum and minimum unsteady temperatures at midspan of rotor pressure surface (eight hot streaks).

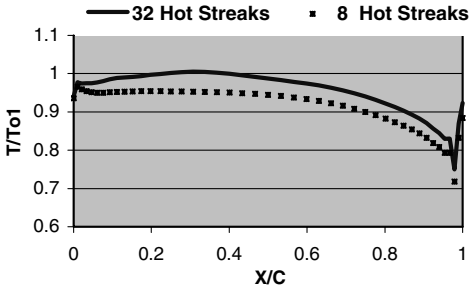

Fig. 13 Time-averaged temperatures at midspan section of rotor pressure surface (NGV midpassage hot streaks).

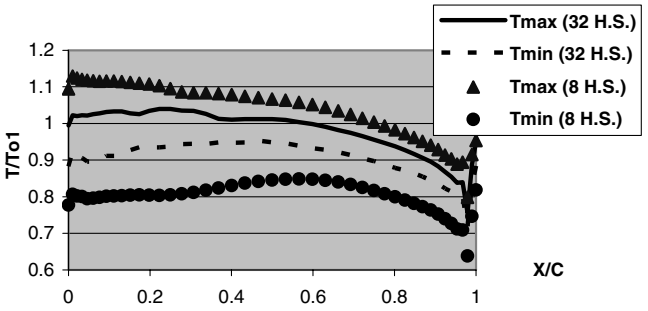

Fig. 14 Maximum and Minimum unsteady temperatures at midspan section of rotor pressure surface (hot streaks are located at the NGV midpassage).

the same inlet temperature distortion magnitude (OTDF and RTDF). The longer residence time for the long-wavelength case with eight hot streaks generates a much larger unsteady response. It is also noted that the maximum unsteady temperature for the eight-hot-streak case is about 8–10% higher than that with 32 hot streaks (Fig. 14). The maximum temperature should be relevant to blade thermal fatigue life. This marked influence of the circumferential wavelength/number of hot streaks on the rotor blade heat load is certainly relevant, because realistic industrial gas turbines typically have six or eight combustion burners. Hence, the clocking characteristics gathered from a configuration in which the number of hot streak is taken to be the same as that of NGV blades may not be applicable to situations with fewer hot streaks.

C. Rotor Blade Forcing

Given that the rotor incidence changes with the hot streak, the associated unsteady loading needs to be examined for blade aeromechanical design considerations.

The frequency spectra of unsteady tangential forces on rotor blades are shown in Fig. 15 for the cases calculated. For the case with 32 hot streaks, the frequency of the hot streaks is the same as the NGV blade passing frequency (i.e., 32 events per revolution). The influence of the hot streaks on unsteady forcing can thus be qualitatively measured by comparing the force amplitudes (Fig. 15b) with those of a uniform inlet (Fig. 15a). The results show that the extra unsteady forcing contributed by the hot streaks is very small, in a region of around 1% of the time-averaged force. The differences in higher harmonics of the fundamental hot-streak/blade passing frequency are also proportionally small. This is in line with previous research showing a relatively small hot-streak influence on the rotor pressure field. The corresponding temperature field is largely driven passively by the passage velocity field in both the NGV and rotor rows.

However, we have a very different picture for the case with eight hot streaks. The unsteady forcing due to the hot streak is indicated by the peak at a frequency of eight per revolution (Fig. 15c). Now the force amplitude due to the hot streak is about 8% of the time-averaged tangential force, significantly larger than that with 32 hot streaks. It is also noted that apart from the two primary disturbances (the hot streak at eight per revolution and the NGV at 32 per

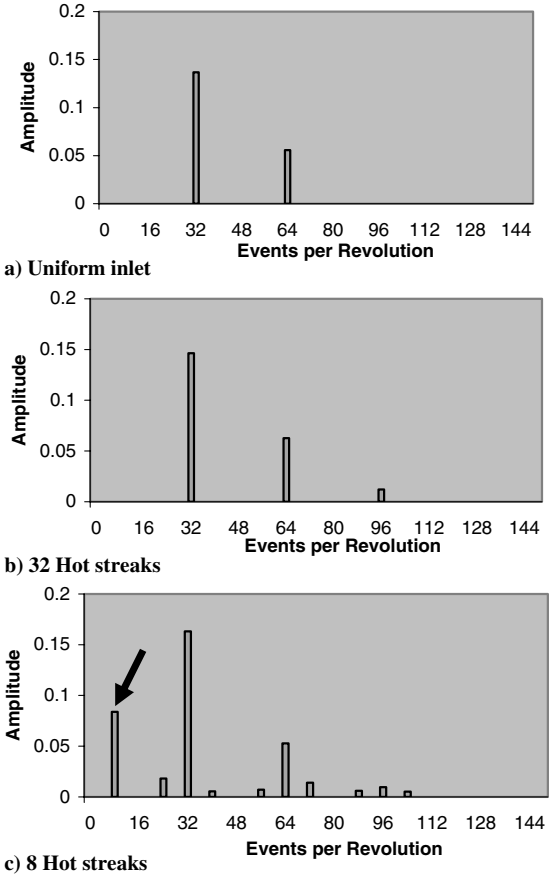

Fig. 15 Spectrum of tangential force amplitude on rotor blades (normalized by the time-averaged value).

revolution) and their higher harmonics, the subharmonics due to the cross-coupling/nonlinear interaction between the two primary disturbances (i.e., components at frequencies of $m\,\omega_{\mathrm{NGV}} + n\,\omega_{\mathrm{hot\ streak}}$ for any integers m and n) also show up on the spectrum. Nevertheless, the relatively small magnitudes of the subharmonics suggest that the unsteady flow responses are still largely linear. It should be noted that the chief difference between the 8- and 32-hot-streak cases is in the time and spatial length scales. For the present eight-hot-streak case, the frequency of the hot streaks is four times lower, and hence a rotor passage should have much more time to respond. The enhanced interactions are thought to be mainly responsible for the much higher forcing at the hot-streak passing frequency (four per revolution), and also for the apparently enhanced forcing at the NGV passing frequency, which is now the fourth harmonic of the fundamental harmonics of hot streaks. In addition, the longer circumferential length scale in the eight-hot-streak case would also be expected to enhance the axial propagation of the convective disturbances, similar to the previous observation for turbine stages subject to a partial admission [10].

Finally, it should be commented that the calculated rotor blade forcing shows little dependency on the hot-streak/NGV clocking for eight-hot-streak cases. This is similar to the temperatures (Figs. 11 and 12). For the case with 32 hot streaks, on the other hand, the clocking effect on the unsteady forcing is also shown to be insignificant, simply because the magnitude of the forcing component attributed to the hot streak with a short wavelength is very small.

IV. Conclusions

The present analysis of hot streaks of the same distortion magnitude but different circumferential length scales reveals a significant influence on both blade forcing and heat load on the turbine rotor.

When the number of hot streaks is the same as that of NGV blades, the rotor blade heat load is strongly dependent on the hot-streak/NGV clocking, giving a maximum difference of 8% in time-averaged temperature on the rotor pressure surface. The unsteady pressure and force on rotor blades, however, are largely unaffected by the hot streaks. The temperature migration inside the rotor row is dictated by the phasing among several cross-passage motions associated with NGV wakes (negative jet), hot-streak heating (positive jet), and NGV and rotor passage secondary flows.

For the case with eight hot streaks, the hot-streak/NGV clocking is shown to have very little effect on rotor surface temperature distributions. The time-averaged temperature on the pressure surface is around 5% lower than that for 32 hot streaks located at the NGV midpassage. However, the unsteady temperature fluctuation is much larger, with the maximum temperature being 8–10% higher than that for 32 hot streaks. Regarding blade aeromechanics, the unsteady forcing on the rotor blades due to the hot streaks is at least five times higher than that with 32 hot streaks. The marked differences in both unsteady forcing and surface temperature between the two cases imply that the number of combustor/burners might be used as a design variable for HP turbine blade aeromechanics as well as heat transfer.

Acknowledgments

The work is sponsored by Siemens Industrial Turbomachinery, Ltd. The authors would like to thank Gurnam Singh (ALSTOM) for providing the baseline computational mesh and Kam Chana (QinetiQ) for providing the experimental data for the MT1 stage.

References

[1] Kerrebrock, J. L., and Mikolajczak, A. A., "Intra-Stator Transport of Rotor Wakes and Its Effect on Compressor Performance," *Journal of Engineering for Gas Turbines and Power*, Vol. 92, No. 4, Oct. 1970, pp. 359–370.

[2] Butler,T. L., Sharma, O. P., Jopslyn, H. D., and Dring, R. P. "Redistribution of Inlet Temperature Distortion in an Axial Flow Turbine Stage," *Journal of Propulsion and Power*, Vol. 5, No. 1, Jan. 1989, pp. 64–71.

[3] Dorney, D. J., Davis R. L., Edwards, D. E., and Madavan, N. K., "Unsteady Analysis of Hot-Streak Migration in a Turbine Stage," *Journal of Propulsion and Power*, Vol. 8, No. 2, Mar. 1992, pp. 520–529.

[4] Krouthen, B., and Giles, M. B., "Numerical Investigation of Hot-Streaks in a Turbine Stage," *Journal of Propulsion and Power*, Vol. 6, No. 6, May, 1990, pp. 769–776.

[5] Shang, T., and Epstein, A. H., "Analysis of Hot Streak Effects on Turbine Rotor Heat Load," *Journal of Turbomachinery*, Vol. 119, No. 3, Apr. 1997, pp. 544–553.

[6] Sondak, D. L., Gupta, V., Orkwis P. D., and Dorney, D. J., "Effects of Blade Count on Linearized and Nonlinear Hot Streak Clocking Simulations," *Journal of Propulsion and Power*, Vol. 18, No. 6, Nov. 2002, pp. 1273–1279.

[7] Dorney, D. J., and Gundy-Burlet, K. L., "Hot Streak Clocking Effects in a 1-1/2 Stage Turbine," *Journal of Propulsion and Power*, Vol. 12, No. 3, May 1996, pp. 619–620.

[8] Takahashi, R. K., Ni, R. H., Sharma, O. P., and Staubach, J. B., "Effects of Hot-Streak Indexing on a 1-1/2 Stage Turbine," AIAA Paper 96-2796, July 1996.

[9] Manwaring, S. R., and Kirkeng, K. L., "Forced Response Vibrations of a Low Pressure Turbine Due to Circumferential Temperature Distortions," *Unsteady Aerodynamics and Aeroelasticity of Turbomachines*, edited by T. Fransson, Kluwer Academic, Dordrecht, The Netherlands, 1998.

[10] He, L., "Computation of Unsteady Flows Through Steam Turbine Blade Rows at Partial Admission," *Proceedings of the Institution of Mechanical Engineers, Part A: Journal of Power and Energy*, Vol. 211, No. 3, Sept. 1997, pp. 197–205.

[11] He, L., "Three-Dimensional Unsteady Navier–Stokes Analysis of Stator-Rotor Interaction in Axial-Flow Turbines," *Proceedings of the Institution of Mechanical Engineers, Part A: Journal of Power and Energy*, Vol. 214, No. 1, Feb. 2000, pp. 13–22.

[12] He, L., Chen, T., Wells, R. G., Li, Y. S. and Ning, W., "Analysis of Rotor-Rotor and Stator-Stator Interferences in Multi-Stage Turbomachines," *Journal of Turbomachinery*, Vol. 124, No. 4, Oct. 2002, pp. 564–571.

[13] Moffatt, S., Ning, W., Li, Y. S., Wells, R. G., and He, L., "Blade Forced Response Prediction for Industrial Gas Turbines," *Journal of Propulsion and Power*, Vol. 21, No. 4, July–Aug. 2005, pp. 707–714.

[14] Jameson, A., "Time-Dependent Calculations Using Multi-Grid, with Applications to Unsteady Flows Past Airfoil and Wings," AIAA Paper 91-1596, Jan. 1991.

[15] Chana, K. S., Povey, T., and Jones, T. V., "Heat Transfer and Aerodynamics of Intermediate Pressure Nozzle Guide Vane with and Without Inlet Temperature Non-Uniformity," American Society of Mechanical Engineers Paper GT 2003-38466, June 2003.

[16] Miller, R. J., Moss, R. W., Ainsworth, R. W., and Harvey, N. W.,"Time-Resolved Vane-Rotor-Vane Interaction in a Transonic One-and-a-Half Stage Turbine," *Proceedings of the Institution of Mechanical Engineers, Part A: Journal of Power and Energy*, Vol. 215, No. 6, Dec. 2001, pp. 675–685.

[17] Povey, T., Chana, K. S., Jones, T. V., and Hurrion, J., "The Effect of Hot-Streaks on HP Vane Surface and Endwall Heat Transfer: An Experimental and Numerical Study," *Journal of Turbomachinery*, Vol. 129, No. 1, Jan. 2007, pp. 32–43.

A. Prasad
Associate Editor